

TOWARDS C^0 FINITE ELEMENT METHODS FOR FOURTH-ORDER ELLIPTIC EQUATION. PART I: GENERAL BOUNDARY CONDITIONS

XIAO ZHANG*, HENGGUANG LI†, NIANYU YI‡, AND PEIMENG YIN§

Abstract. This paper is part of a series developing C^0 finite element methods for fourth-order elliptic equations on polygonal domains. Here, we investigate how boundary conditions influence the design of effective C^0 schemes, specifically focusing on equations without lower-order terms, namely the biharmonic equation. We propose a modified mixed formulation that decomposes the problem into a system of Poisson equations, where the number of equations depends on both the largest interior angle and the boundary conditions on its two adjacent sides. In contrast to the naive mixed formulation, which involves only two Poisson problems, the proposed approach guarantees convergence to the true solution for arbitrary polygonal domains and general boundary conditions, including Navier, Neumann, and mixed boundary conditions. C^0 finite element algorithms are developed, rigorous error estimates are established, and numerical experiments are presented to demonstrate the well-posedness and effectiveness of the proposed method.

Key words. biharmonic equation, general boundary conditions, mixed formulation, C^0 finite element method, error estimate.

MSC codes. 65N12, 65N30, 35J40

1 Introduction Let $\Omega \subset \mathbb{R}^2$ be a polygonal domain whose boundary is decomposed as $\partial\Omega = \bar{\Gamma}_D \cup \bar{\Gamma}_N$, where Γ_D and Γ_N are two disjoint open subsets of $\partial\Omega$. Given $f \in L^2(\Omega)$, we are interested in developing C^0 finite element algorithms for the following fourth-order elliptic problem:

$$(1.1) \quad \begin{cases} \Delta^2 u - b\Delta u + cu = f, & \text{in } \Omega, \\ u = \Delta u = 0, & \text{on } \Gamma_D, \\ \partial_{\mathbf{n}} u = \partial_{\mathbf{n}} \Delta u = 0, & \text{on } \Gamma_N. \end{cases}$$

Here, b and c are nonnegative constants, and \mathbf{n} denotes the outward unit normal vector on $\partial\Omega$. The boundary segments Γ_D and Γ_N correspond to Dirichlet and Neumann boundary conditions, respectively.

To develop C^0 finite element methods for the biharmonic equation with Navier boundary conditions, a typical approach is to reformulate the problem as a fully decoupled system of lower-order elliptic equations, which allows for the direct use of C^0 finite element spaces [24]. However, due to the presence of lower-order terms in (1.1), the equation cannot be rewritten as a fully decoupled system. Consequently, existing C^0 finite element methods with correction techniques for the biharmonic equation under Navier boundary conditions cannot be directly extended to problem (1.1).

In a series of works, we aim to develop C^0 finite element methods for problem (1.1). In the present paper, we first focus on the influence of boundary conditions on C^0 finite element methods for biharmonic problem, namely the case $b = c = 0$ in (1.2):

$$(1.2) \quad \begin{cases} \Delta^2 u = f, & \text{in } \Omega, \\ u = \Delta u = 0, & \text{on } \Gamma_D, \\ \partial_{\mathbf{n}} u = \partial_{\mathbf{n}} \Delta u = 0, & \text{on } \Gamma_N. \end{cases}$$

The biharmonic problem has been extensively studied in fields such as fluid mechanics and structural mechanics [25, 32, 34, 37, 38], where different types of boundary conditions correspond to specific application scenarios. For the boundary conditions defined in problem (1.2), when $\Gamma_D = \partial\Omega$, the

*School of Mathematics and Computational Science, Xiangtan University, Xiangtan 411105, P.R.China (202431510169@mail.xtu.edu.cn)

†Department of Mathematics and Institute for AI and Data Science, Wayne State University, Detroit, Michigan, USA (li@wayne.edu).

‡Hunan Key Laboratory for Computation and Simulation in Science and Engineering; School of Mathematics and Computational Science, Xiangtan University, Xiangtan 411105, P.R.China (yinianyu@xtu.edu.cn).

§Corresponding author. Department of Mathematical Sciences, The University of Texas at El Paso, El Paso, TX 79968, USA (pyin@utep.edu).

problem is said to satisfy Navier boundary conditions [13, 35]. This case arises in structural mechanics, for instance in models describing the static loading of a thin plate with hinged boundaries. In contrast, when $\Gamma_N = \partial\Omega$, the problem is referred to as the Neumann boundary condition case [26]. Problems of this type are associated with physical models such as the transverse vibration of a thin plate with free boundaries and the natural deformation of membrane materials [11].

In this paper, we treat the cases $\Gamma_D = \partial\Omega$ and $\Gamma_N = \partial\Omega$ as trivial cases of mixed boundary conditions. In general, Γ_D and Γ_N may be nontrivial subsets of $\partial\Omega$, thereby encompassing a broader class of physical models. For such fourth-order problems, finite element methods based on direct variational formulations can be employed [2]. Typical choices include C^1 finite elements, such as the Argyris element, which consists of fifth-degree polynomials [36], and the Morley element, a quadratic nonconforming element [22]. However, the construction of these finite element spaces is often complicated, making the corresponding methods challenging to implement in practice. Alternative approaches, including discontinuous Galerkin methods [17] and the C^0 interior penalty Galerkin method [4, 5], are also viable. Nevertheless, the choice of penalty parameters is often subtle. For the biharmonic equation with Navier or Dirichlet boundary conditions, the problem can be decomposed into a system of Poisson equations and a Stokes equation [16, 21]. However, such a decomposition is no longer applicable when the fourth-order elliptic equation includes lower-order terms.

Motivated by the structure of the boundary conditions in problem (1.2), an intuitive strategy is to decouple the biharmonic problem into a system of Poisson equations, which can then be efficiently solved using standard finite element methods. Mixed finite element methods based on C^0 finite elements offer an attractive framework for the numerical approximation of the biharmonic problem (1.2) [1, 6–9, 15, 21, 24, 28]. A large portion of the existing literature focuses on clamped boundary conditions (also referred to as Dirichlet boundary conditions), namely ($u = \partial_n u = 0$ on $\partial\Omega$) [14, 20, 21, 33]. For biharmonic problems with Navier boundary conditions, it has been observed [12, 18, 24, 31, 39] that when the domain Ω is nonconvex, the mixed finite element solution of problem (1.2) may fail to coincide with the true solution for certain source terms $f \in L^2(\Omega)$. This discrepancy is known as the Sapongyan paradox [30, 39]. This arises because the function space of the solution to a mixed variational problem may not coincide with that of the corresponding direct variational problem, owing to the presence of a low-regularity term that does not belong to $H^2(\Omega)$ [29, 39].

Recently, a modified mixed formulation was proposed in [24] for the biharmonic equation with Navier boundary conditions. This formulation decomposes the problem into a system of three Poisson equations, in which an additional intermediate Poisson problem is introduced to ensure that the solution is confined to the correct function space. A similar phenomenon was further observed for the triharmonic equation with simply supported boundary conditions [23], which can be naively decomposed into three Poisson equations with Dirichlet boundary conditions. However, the solutions obtained from these Poisson equations may still lie in a larger function space, resulting in weak solutions that exhibit behavior similar to the Sapongyan paradox. To address this issue, one to three additional Poisson equations, depending on the largest interior angle, may be introduced to further confine the solution to the correct function space.

Existing C^0 finite element algorithms for the biharmonic equation are largely restricted to Navier boundary conditions. To develop an effective C^0 finite element algorithm for (1.1), it is crucial to investigate how general boundary conditions influence the convergence of the C^0 finite element approximation. From this perspective, the Navier case can be viewed as a special instance. By analyzing the orthogonal complement of the range of the Laplace operator mapping H^2 , equipped with appropriate boundary conditions, into $L^2(\Omega)$, we first construct a modified decoupled scheme for problem (1.2). This scheme transforms the biharmonic problem into a system of three or four Poisson problems, in which the number of equations depends on the largest interior angle of the domain (possibly including angles greater than $\frac{\pi}{2}$), as well as on the specific choice of boundary conditions. In addition to the two Poisson problems directly arising from the biharmonic problem, a varying number of additional Poisson problems is required to ensure that the solution is confined to the correct Sobolev space. In particular, if only one interior angle exceeds $\frac{\pi}{2}$, then at most one additional Poisson problem is needed for Navier or Neumann boundary conditions, whereas up to two additional Poisson problems are required for mixed boundary conditions. A theoretical analysis is presented to demonstrate the

equivalence between the proposed mixed formulation, that is, the system of Poisson problems, and the original biharmonic problem in appropriate Sobolev spaces. Each of these Poisson problems can be solved using standard finite element methods, thereby forming a hybrid finite element algorithm for the biharmonic problem (1.2). In this way, the numerical solution of problem (1.2) via the resulting system of Poisson problems becomes both simple and efficient.

To solve the proposed mixed formulation, we develop a numerical algorithm using piecewise linear C^0 finite elements. In addition, we provide an error analysis for the finite element approximations of both the auxiliary function w and the solution u . For the auxiliary function w , the error in the H^1 norm is standard and converges at a rate of h^α on a quasi-uniform mesh, where α depends on the largest interior angle and the boundary conditions on both sides of that angle. The L^2 error estimate is derived using a standard duality argument. For the solution u , the approximation has a convergence rate of $h^{\min\{1,2\alpha\}}$ in general. For Navier and Neumann boundary conditions, the optimal convergence rate is h^1 , whereas for mixed boundary conditions, the convergence rate is h^1 if the interior angle is no more than π and $h^{2\alpha}$ if the angle is greater than π . Numerical examples are presented to compare the proposed method with existing numerical approaches, such as the C^0 interior penalty method. The solutions obtained from the proposed C^0 finite element algorithm agree very well with those computed using the C^0 interior penalty method [4, 5]. The observed numerical convergence rates are in good agreement with the theoretical predictions.

The remainder of the paper is organized as follows. In [Section 2](#), drawing on the theory for second-order elliptic equations developed in [19], we identify the deficiencies of the solution space associated with the naive decoupled formulation. We then characterize the dimension of the orthogonal complement of the image of the Laplace operator and construct a corresponding basis. Based on these results, we propose a modified scheme and establish its well-posedness. In [Section 3](#), we present a mixed finite element algorithm for the modified scheme and derive error estimates for both the primary solution and the auxiliary function on quasi-uniform meshes. The extension to Neumann boundary conditions is discussed in [Section 4](#). Finally, in [Section 5](#), we report numerical experiments on a range of representative polygonal domains and boundary conditions to verify the effectiveness of the proposed scheme.

2 Biharmonic problem with mixed boundary conditions Let $\gamma = (\gamma_1, \dots, \gamma_d) \in \mathbb{Z}_{\geq 0}^d$ be a multi-index, and define $\partial^\gamma := \partial_{x_1}^{\gamma_1} \cdots \partial_{x_d}^{\gamma_d}$, $|\gamma| := \sum_{i=1}^d \gamma_i$. For $m \geq 0$, the Sobolev space $H^m(\Omega)$ consists of functions whose weak derivatives up to order m are square-integrable. In particular, $L^2(\Omega) := H^0(\Omega)$. For $s > 0$, let $s = m + t$ with $m \in \mathbb{Z}_{\geq 0}$ and $0 < t < 1$. For $D \subseteq \mathbb{R}^d$, the fractional Sobolev space $H^s(D)$ consists of distributions v in D such that

$$\|v\|_{H^s(D)}^2 := \|v\|_{H^m(D)}^2 + \sum_{|\gamma|=m} \int_D \int_D \frac{|\partial^\gamma v(x) - \partial^\gamma v(y)|^2}{|x-y|^{d+2t}} dx dy < \infty.$$

The norm $\|\cdot\|_{H^s(\Omega)}$ is abbreviated as $\|\cdot\|_s$ for $s > 0$, and $\|\cdot\|_{L^2(\Omega)}$ is abbreviated as $\|\cdot\|$. We define $H_0^s(D)$ as the closure of $C_0^\infty(D)$ in $H^s(D)$, $H^{-s}(D)$ as the dual space of $H_0^s(D)$, $\tilde{H}^s(D)$ as the space of all functions v on D whose extension \tilde{v} by zero outside D belongs to $H^s(\mathbb{R}^d)$, and $\tilde{H}^{-s}(D)$ as the dual space of $\tilde{H}^s(D)$. In addition, we use the notation $a \lesssim b$ for quantities a, b to mean $a \leq Cb$, where $C > 0$ is a constant depending only on Ω and the boundary conditions.

In this section, we consider problem (1.2) under the assumption that $\Gamma_D \neq \emptyset$. The special case where $\Gamma_N = \partial\Omega$ will be addressed in [Section 4](#). We define the Sobolev space

$$(2.1) \quad V^2 := \{v \in H^2(\Omega) : v|_{\Gamma_D} = 0, \partial_{\mathbf{n}} v|_{\Gamma_N} = 0\}.$$

The variational formulation of problem (1.2) is then: find $u \in V^2$ such that

$$(2.2) \quad a(u, v) = (f, v), \quad \forall v \in V^2,$$

where the bilinear form $a(u, v)$ is defined by

$$(2.3) \quad a(u, v) := \int_{\Omega} \Delta u \Delta v \, dx.$$

For any $u, v \in V^2$, the bilinear form $a(u, v)$ is continuous on V^2 :

$$|a(u, v)| = \left| \int_{\Omega} \Delta u \Delta v \, dx \right| \leq \|\Delta u\| \|\Delta v\| \leq \|u\|_2 \|v\|_2.$$

For any $u \in V^2$, the coercivity of $a(u, u)$ follows from the inequality [19, Theorem 2.2.3]:

$$\|u\|_2^2 \lesssim \|\Delta u\|^2 = a(u, u).$$

Therefore, the Lax–Milgram Theorem guarantees that the variational problem (2.2) is well-posed.

2.1 Naive mixed formulation The problem (1.2) can be decoupled into two Poisson problems with mixed boundary conditions

$$(2.4) \quad \begin{cases} -\Delta w = f & \text{in } \Omega, \\ w = 0 & \text{on } \Gamma_D, \\ \partial_{\mathbf{n}} w = 0 & \text{on } \Gamma_N, \end{cases} \quad \text{and} \quad \begin{cases} -\Delta \bar{u} = w & \text{in } \Omega, \\ \bar{u} = 0 & \text{on } \Gamma_D, \\ \partial_{\mathbf{n}} \bar{u} = 0 & \text{on } \Gamma_N, \end{cases}$$

which is referred to as the naive mixed formulation. Define the Sobolev space

$$V^1 := \{v \in H^1(\Omega) : v|_{\Gamma_D} = 0\},$$

Then the corresponding variational form for (2.4) is to find $\bar{u}, w \in V^1$ such that

$$(2.5) \quad \begin{cases} A(w, \phi) = (f, \phi), & \forall \phi \in V^1, \\ A(\bar{u}, \psi) = (w, \psi), & \forall \psi \in V^1, \end{cases}$$

where the bilinear form

$$(2.6) \quad A(\phi, \psi) := \int_{\Omega} \nabla \phi \cdot \nabla \psi \, dx.$$

This decoupled system consists of two standard Poisson problems, each of which is well posed and admits a unique solution under mixed boundary conditions, provided that $\Gamma_D \neq \emptyset$. Given $f \in H^{-1}(\Omega)$, the variational problem (2.5) admits a weak solution $(\bar{u}, w) \in V^1 \subset H^1(\Omega)$. Since the solution u to the original problem (1.2) belongs to V^2 , it is natural to question whether the solution \bar{u} from the mixed formulation (2.4) also lies in V^2 . If not, then \bar{u} cannot be regarded as the true solution to the original biharmonic problem (1.2).

Navier boundary conditions, i.e., $\Gamma_D = \partial\Omega$, the equivalence between the mixed formulation (2.4) and the original biharmonic problem has been studied in [24]. It was shown that, in domains with reentrant corners, the solution of the mixed formulation (2.4) does not belong to the same Sobolev space as the solution of the biharmonic problem (1.2), a phenomenon known as the Saponyan paradox [29, 39]. For biharmonic problems with mixed boundary conditions as in (1.2), a similar discrepancy also arises for the solution of the mixed formulation (2.4). In the following, we analyze the solution structure in detail and develop effective methods to address this issue.

2.2 Modified mixed formulation For the biharmonic problem (1.2), we allow interior angles equal to π at points where different types of boundary conditions meet, and we regard each such boundary transition point as a vertex of the polygonal domain Ω for analytical purposes. Then each edge of Ω lies entirely in either $\bar{\Gamma}_D$ or $\bar{\Gamma}_N$.

DEFINITION 2.1 (Vertex, edge, and indicator sets). *Let $\{Q_j\}_{j=1}^n$ denote the vertices of $\partial\Omega$, ordered counterclockwise, with interior angles ω_j . For each j , let the open set Γ_j be the edge connecting Q_{j-1} and Q_j ($Q_0 = Q_n$), so that $\partial\Omega = \bigcup_{j=1}^n \Gamma_j$. For a vertex Q_j , the index j is classified according to the boundary conditions on the adjacent edges Γ_j and Γ_{j+1} as the following indicator sets:*

- \mathcal{D}^2 : $\Gamma_j, \Gamma_{j+1} \subset \Gamma_D$;
- \mathcal{N}^2 : $\Gamma_j, \Gamma_{j+1} \subset \Gamma_N$;

- \mathcal{M}' : $\Gamma_j \subset \Gamma_N$, $\Gamma_{j+1} \subset \Gamma_D$;
- \mathcal{M}'' : $\Gamma_j \subset \Gamma_D$, $\Gamma_{j+1} \subset \Gamma_N$.

For the convenience of analysis, we impose the following assumptions throughout the paper:

ASSUMPTION 2.2. (i) All interior angles of Ω are at most $\frac{\pi}{2}$, except for the largest interior angle $\omega := \omega_\ell$ at the vertex $Q := Q_\ell$, where $1 \leq \ell \leq n$. In other words, we consider a polygon with at most a single vertex that gives rise to the Saponyan paradox. (ii) Dirichlet boundary conditions are imposed on all boundary edges except for the two edges adjacent to Q . The boundary conditions on Γ_ℓ and $\Gamma_{\ell+1}$ as shown in [Figure 1](#) will be specified later. Equivalently,

$$(2.7) \quad \tilde{\Gamma} := \partial\Omega \setminus (\bar{\Gamma}_\ell \cup \bar{\Gamma}_{\ell+1}) \subset \bar{\Gamma}_D.$$

Position the vertex Q at the origin and align its adjacent edge $\Gamma_{\ell+1}$ with the positive horizontal axis. Let (r, θ) denote the polar coordinates. Then Ω lies within the cone bounded by $\theta = 0$ and $\theta = \omega$. Define the sector

$$K_\omega^R := \{(r \cos \theta, r \sin \theta) \in \Omega \mid (r, \theta) \in (0, R) \times (0, \omega)\},$$

where R is chosen so that $K_\omega^R \subset \Omega$. A schematic of the domain and the sector is shown in [Figure 1](#).

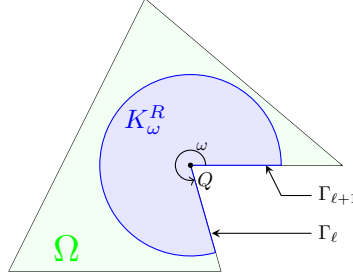


Figure 1: Ω and K_ω^R .

2.2.1 L^2 basis function The Laplace operator $\Delta : V^2 \rightarrow L^2(\Omega)$ is injective, and its range $\mathcal{S} := \Delta(V^2)$ forms a closed subspace of $L^2(\Omega)$ with finite codimension [19]. Let \mathcal{S}^\perp denote the orthogonal complement of \mathcal{S} in $L^2(\Omega)$. Then one has the orthogonal decomposition $\mathcal{S} \oplus \mathcal{S}^\perp = L^2(\Omega)$. \mathcal{S}^\perp is not necessarily empty. For a polygon, if $\omega < \frac{\pi}{2}$, we have $\mathcal{S} = L^2(\Omega)$, and the solution of the Poisson problem belongs to V^2 whenever the source term is in $L^2(\Omega)$. However, if the index $\ell \in \mathcal{D}^2$ and $\omega > \pi$, it has been shown that $\dim(\mathcal{S}^\perp) = 1$ [19, 24], i.e., $\mathcal{S} \subsetneq L^2(\Omega)$. In this case, in general $\mathcal{S} \not\subseteq L^2(\Omega)$, which implies that the solution \bar{u} obtained from the mixed formulation (2.4) does not lie in V^2 . When the index ℓ belongs to other indicator sets defined in [Definition 2.1](#), situations where $\mathcal{S} \not\subseteq L^2(\Omega)$ may also occur, depending on the largest interior angle ω and the type of indicator set. Analogous to the case $\ell \in \mathcal{D}^2$, the orthogonal complement \mathcal{S}^\perp for all other cases is finite-dimensional, with an explicitly determinable basis.

DEFINITION 2.3. At vertex Q , we define the functions $\xi_m = \xi_m(r, \theta; \tau, R) \in L^2(\Omega)$ by

$$(2.8) \quad \xi_m := \chi s_m + \zeta_m,$$

where the cut-off function $\chi = \chi(r; \tau, R) \in C^\infty(\Omega)$ satisfies

$$\chi(r; \tau, R) = \begin{cases} 1, & 0 \leq r \leq \tau R, \\ 0, & r \geq R, \end{cases}$$

$s_m = s_m(r, \theta) \in L^2(\Omega)$ depends on indicator at Q and the interior angle ω ,

$$(2.9) \quad s_m := \begin{cases} r^{-\frac{\pi}{\omega}} \sin\left(\frac{\pi}{\omega}\theta\right), & \ell \in \mathcal{D}^2, \omega \in (\pi, 2\pi), m = 1, \\ r^{-\frac{\pi}{\omega}} \cos\left(\frac{\pi}{\omega}\theta\right), & \ell \in \mathcal{N}^2, \omega \in (\pi, 2\pi), m = 1, \\ r^{-\frac{\pi}{2\omega}} \sin\left(\frac{\pi}{2\omega}\theta\right), & \ell \in \mathcal{M}', \omega \in \left(\frac{\pi}{2}, \frac{3\pi}{2}\right], m = 1, \\ r^{-\frac{(2m-1)\pi}{2\omega}} \sin\left(\frac{(2m-1)\pi}{2\omega}\theta\right), & \ell \in \mathcal{M}', \omega \in \left(\frac{3\pi}{2}, 2\pi\right), m = 1, 2, \\ r^{-\frac{\pi}{2\omega}} \cos\left(\frac{\pi}{2\omega}\theta\right), & \ell \in \mathcal{M}'', \omega \in \left(\frac{\pi}{2}, \frac{3\pi}{2}\right], m = 1, \\ r^{-\frac{(2m-1)\pi}{2\omega}} \cos\left(\frac{(2m-1)\pi}{2\omega}\theta\right), & \ell \in \mathcal{M}'', \omega \in \left(\frac{3\pi}{2}, 2\pi\right), m = 1, 2, \end{cases}$$

and $\zeta_m \in H^1(\Omega)$ is defined as the variational solution of the Poisson problem

$$(2.10) \quad \begin{cases} -\Delta \zeta_m = \Delta(\chi s_m) & \text{in } \Omega, \\ \zeta_m = 0 & \text{on } \Gamma_D, \\ \partial_{\mathbf{n}} \zeta_m = 0 & \text{on } \Gamma_N. \end{cases}$$

By the cut-off function χ , it follows

$$\chi s_m = \partial_{\mathbf{n}}(\chi s_m) = 0 \quad \text{on } \tilde{\Gamma}.$$

The definition of s_m in (2.9) implies that for $j = \ell, \ell + 1$,

$$(2.11) \quad \begin{cases} \chi s_m|_{\Gamma_j} = 0 & \text{if } \Gamma_j \subset \Gamma_D, \\ \partial_{\mathbf{n}}(\chi s_m)|_{\Gamma_j} = 0 & \text{if } \Gamma_j \subset \Gamma_N. \end{cases}$$

Furthermore, we observe that

$$\Delta(\chi s_m)|_{K_{\omega}^{\tau R} \cup (\Omega \setminus K_{\omega}^R)} = 0, \quad \Delta(\chi s_m) \in C^{\infty}(K_{\omega}^R \setminus K_{\omega}^{\tau R}),$$

which implies $\Delta(\chi s_m) \in L^2(\Omega)$. By elliptic regularity for (2.10), it holds $\zeta_m \in H^1(\Omega)$.

We introduce the maximal extension of the Laplace operator Δ in $L^2(\Omega)$:

$$D(\Delta, L^2(\Omega)) = \{v \in L^2(\Omega); \Delta v \in L^2(\Omega)\}.$$

For a function v , let $\gamma_j v$ be the restriction of v to Γ_j .

LEMMA 2.4. [19, Theorem 1.5.2] Let Ω be an open polygonal subset of \mathbb{R}^2 . Then the mapping

$$v \mapsto \{\gamma_j v, \gamma_j(\partial v / \partial n)\},$$

which is defined for $H^2(\Omega)$ has an unique continuous extension as an operator from $D(\Delta, L^2(\Omega))$ into $\tilde{H}^{-1/2}(\Gamma_j) \times \tilde{H}^{-3/2}(\Gamma_j)$.

Therefore, the function ξ_m in (2.8) has the following properties.

LEMMA 2.5. (i) ξ_m depends on r, θ , but are independent of τ, R . That is, for any two distinct parameter pairs (τ_l, R_l) , $l = 1, 2$, satisfying $\min\{\tau_1 R_1, \tau_2 R_2\} > \delta > 0$, it follows

$$\xi_m(r, \theta; \tau_1, R_1) = \xi_m(r, \theta; \tau_2, R_2).$$

(ii) The function $\xi_m \in D(\Delta, L^2(\Omega))$ is uniquely defined and satisfies

$$(2.12) \quad \begin{cases} -\Delta \xi_m = 0 & \text{in } \Omega, \\ \xi_m = 0 & \text{on } \Gamma_D, \\ \partial_{\mathbf{n}} \xi_m = 0 & \text{on } \Gamma_N. \end{cases}$$

Proof. The proof of (i) is analogous to Lemma 2.4 in [24], while that of (ii) follows from Lemma 2.3.6 in [19]. \square

Since $\xi_m(r, \theta; \tau, R)$ is independent of τ and R (see Lemma 2.5), we may simply write

$$\xi_m(r, \theta) := \xi_m(r, \theta; \tau, R).$$

2.2.2 Orthogonal space of the Laplace operator image We explicitly characterize the orthogonal complement \mathcal{S}^\perp . We begin by identifying the possible components contained in it.

LEMMA 2.6. *The function ξ_m defined in (2.8) belongs to \mathcal{S}^\perp . In particular, for $\ell \in \mathcal{M}' \cup \mathcal{M}''$ and $\omega \in (3\pi/2, 2\pi)$, the functions ξ_m , $m = 1, 2$, are linearly independent.*

Proof. For any $v \in \mathcal{S}$, there exists $z \in V^2$ such that $-\Delta z = v$. Taking the inner product of v with ξ_m gives

$$\begin{aligned} \int_{\Omega} v \xi_m dx &= \int_{\Omega} -\Delta z \xi_m dx = \int_{\Omega} -z \Delta \xi_m dx + \int_{\partial\Omega} z \partial_{\mathbf{n}} \xi_m - \partial_{\mathbf{n}} z \xi_m ds \\ &= \int_{\Omega} -z \Delta \xi_m dx + \int_{\Gamma_D} -\partial_{\mathbf{n}} z \xi_m ds + \int_{\Gamma_N} z \partial_{\mathbf{n}} \xi_m ds = 0, \end{aligned}$$

where we have used (2.12). Therefore, $\xi_m \in \mathcal{S}^\perp$.

If $\ell \in \mathcal{M}' \cup \mathcal{M}''$ and $\omega \in (3\pi/2, 2\pi)$, suppose that for some constants k_1, k_2 ,

$$k_1 \xi_1 + k_2 \xi_2 = k_1 \zeta_1 + k_2 \zeta_2 + \chi(k_1 s_1 + k_2 s_2) = 0,$$

which implies $\chi(k_1 s_1 + k_2 s_2) = -(k_1 \zeta_1 + k_2 \zeta_2) \in H^1(\Omega)$. Since $s_m \notin H^1(\Omega)$, $m = 1, 2$, it holds

$$(2.13) \quad k_1 s_1 + k_2 s_2 = 0.$$

Multiplying (2.13) by $r^{-\frac{\pi}{2\omega}}$ yields $k_2 r^{-\frac{\pi}{2\omega}} s_2 = -k_1 r^{-\frac{\pi}{2\omega}} s_1 \in L^2(\Omega)$. However, since $r^{-\frac{\pi}{2\omega}} s_2 \notin L^2(\Omega)$, it must be that $k_2 = 0$, and consequently $k_1 = 0$. Hence, ξ_1 and ξ_2 are linearly independent. \square

Regarding the dimension of \mathcal{S}^\perp in a general polygonal domain, we recall the following result.

LEMMA 2.7. [19, Theorem 2.3.7] *Given a general polygonal domain, the dimension of \mathcal{S}^\perp is equal to the cardinality of the set $\{\lambda_{j,m} : 0 < \lambda_{j,m} < 1, m \geq 1\}$, that is,*

$$(2.14) \quad \dim \mathcal{S}^\perp = \text{card}\{\lambda_{j,m} : 0 < \lambda_{j,m} < 1, m \geq 1\}.$$

Here, $\lambda_{j,m}$ ($j = 1, \dots, n$; $m \geq 1$) denote the eigenvalues of the boundary value problem

$$(2.15) \quad -\partial_{\theta}^2 \phi = \lambda^2 \phi, \quad \theta \in (0, \omega_j), \quad \phi \in D_j,$$

where the admissible sets D_j are defined as

$$D_j = \begin{cases} \{\phi \in H^2([0, \omega_j]) : \phi(0) = 0, \phi(\omega_j) = 0\}, & j \in \mathcal{D}^2, \\ \{\phi \in H^2([0, \omega_j]) : \phi'(0) = 0, \phi'(\omega_j) = 0\}, & j \in \mathcal{N}^2, \\ \{\phi \in H^2([0, \omega_j]) : \phi'(0) = 0, \phi(\omega_j) = 0\}, & j \in \mathcal{M}', \\ \{\phi \in H^2([0, \omega_j]) : \phi(0) = 0, \phi'(\omega_j) = 0\}, & j \in \mathcal{M}''. \end{cases}$$

For a general polygonal domain, it can be readily verified that, for a fixed j , the solution of the eigenvalue problem (2.15) is given by

$$\lambda_{j,m} = \begin{cases} m\pi/\omega_j, & j \in \mathcal{D}^2, \\ (m-1)\pi/\omega_j, & j \in \mathcal{N}^2, \\ (m - \frac{1}{2})\pi/\omega_j, & j \in \mathcal{M}' \cup \mathcal{M}'', \end{cases} \quad m = 1, 2, \dots$$

Then, the dimension of \mathcal{S}^\perp in (2.14) reduces to

$$(2.16) \quad d_\perp := \dim \mathcal{S}^\perp = \text{card} \{ j \in \mathcal{D}^2 \cup \mathcal{N}^2 : \omega_j \in (\pi, 2\pi) \} + \text{card} \left\{ j \in \mathcal{M}' \cup \mathcal{M}'' : \omega_j \in \left(\frac{\pi}{2}, \frac{3\pi}{2} \right) \right\} \\ + 2\text{card} \left\{ j \in \mathcal{M}' \cup \mathcal{M}'' : \omega_j \in \left(\frac{3\pi}{2}, 2\pi \right) \right\},$$

which shows that \mathcal{S}^\perp is finite-dimensional, with its dimension determined by the interior angles ω_j and the types of boundary conditions prescribed on the polygonal domain.

Upon revisiting our earlier assumptions, we obtain to the following result.

COROLLARY 2.8. *Under Assumption 2.2, the dimension of the orthogonal space \mathcal{S}^\perp holds*

$$(2.17) \quad d_\perp = \begin{cases} 1, & \ell \in \mathcal{D}^2 \cup \mathcal{N}^2, \omega \in (\pi, 2\pi), \text{ or } \ell \in \mathcal{M}' \cup \mathcal{M}'', \omega \in (\frac{1}{2}\pi, \frac{3}{2}\pi], \\ 2, & \ell \in \mathcal{M}' \cup \mathcal{M}'', \omega \in (\frac{3}{2}\pi, 2\pi). \end{cases}$$

Furthermore, \mathcal{S}^\perp can be expressed as

$$(2.18) \quad \mathcal{S}^\perp = \text{span}_m \{ \xi_m \},$$

where ξ_m , $m = 1, \dots, d_\perp$ is given in (2.8).

Proof. By the definition of ξ_m in (2.8) and Lemma 2.7, it follows $d_\perp = \text{card}_m \{ \xi_m \}$. Additionally, Lemma 2.6 implies $\xi_m \in \mathcal{S}^\perp$, and hence (2.18) holds. \square

2.3 Modified mixed formulation and its well-posedness By Corollary 2.8, any function $w \in L^2(\Omega)$ can be decoupled as

$$(2.19) \quad w = w_{\mathcal{S}} + w_{\mathcal{S}^\perp},$$

where $w_{\mathcal{S}} \in \mathcal{S}$ and $w_{\mathcal{S}^\perp} \in \mathcal{S}^\perp$, satisfying

$$w_{\mathcal{S}^\perp} = \sum_{m=1}^{d_\perp} c_m \xi_m, \text{ and } (w_{\mathcal{S}}, w_{\mathcal{S}^\perp}) = 0.$$

Taking the inner product of both sides of (2.19) with ξ_m yields a linear system for the coefficients:

$$(2.20) \quad \Xi C = W,$$

where $\Xi = [(\xi_m, \xi_{m'})]_{m,m'=1}^{d_\perp} \in \mathbb{R}^{d_\perp \times d_\perp}$ is the associated Gram matrix, $C = [c_m]_{m=1}^{d_\perp} \in \mathbb{R}^{d_\perp}$ is the coefficient vector, and $W = [(w, \xi_m)]_{m=1}^{d_\perp} \in \mathbb{R}^{d_\perp}$ is the right-hand side vector.

LEMMA 2.9. *The linear system (2.20) admits a unique solution.*

Proof. If $d_\perp = 1$, the coefficient is given explicitly by $c_1 = \frac{(w, \xi_1)}{\|\xi_1\|^2}$. If $d_\perp = 2$, by Lemma 2.6, the basis functions ξ_1 and ξ_2 are linearly independent. Therefore, the associated Gram matrix Ξ satisfies

$$|\Xi| = \|\xi_1\|^2 \|\xi_2\|^2 - (\xi_1, \xi_2)^2 > 0,$$

which implies that Ξ is nonsingular. Consequently, the coefficient vector C is uniquely determined. \square

Then the naive mixed formulation (2.4) can be refined into the modified mixed formulation

$$(2.21) \quad \begin{cases} -\Delta w = f & \text{in } \Omega, \\ w = 0 & \text{on } \Gamma_D, \\ \partial_{\mathbf{n}} w = 0 & \text{on } \Gamma_N, \end{cases} \quad \begin{cases} -\Delta \tilde{u} = w_{\mathcal{S}} & \text{in } \Omega, \\ \tilde{u} = 0 & \text{on } \Gamma_D, \\ \partial_{\mathbf{n}} \tilde{u} = 0 & \text{on } \Gamma_N. \end{cases}$$

The corresponding variational formulation seeks $\tilde{u}, w \in V^1$ such that

$$(2.22a) \quad A(w, \phi) = (f, \phi), \quad \forall \phi \in V^1,$$

$$(2.22b) \quad A(\tilde{u}, \psi) = (w_S, \psi), \quad \forall \psi \in V^1,$$

For the modified mix formulation (2.21), we have the following results.

THEOREM 2.10. *For $f \in L^2(\Omega)$, the solution \tilde{u} to the modified variational problem (2.22) is identical to the solution u of the biharmonic problem (2.2), i.e., $\tilde{u} = u \in V^2$.*

Proof. Since $w_S \in \mathcal{S}$, it follows $\tilde{u} \in V^2$. For any $v \in V^2$, one has

$$(\Delta \tilde{u}, \Delta v)_\Omega = (w - w_{S^\perp}, \Delta v)_\Omega = -(w, \Delta v)_\Omega + (w_{S^\perp}, \Delta v)_\Omega = (\nabla w, \nabla v)_\Omega - (w, \partial_n v)_{\partial\Omega}.$$

Since $w \in V^1$, $v \in V^2$, it holds $(w, \partial_n v)_{\partial\Omega} = (w, \partial_n v)_{\Gamma_D} + (w, \partial_n v)_{\Gamma_N} = 0$. Thus,

$$(-\Delta \tilde{u}, \Delta v)_\Omega = (\nabla w, \nabla v)_\Omega = (f, v)_\Omega.$$

Therefore, \tilde{u} satisfies (2.2). By the uniqueness of the solution to (2.2) in V^2 , it holds $\tilde{u} = u$. \square

In the following, we will not distinguish between u and \tilde{u} , and will uniformly denote them as u .

LEMMA 2.11. *The solution (w, u) to the modified mixed formulation (2.22) satisfies*

$$\|w\|_1 \lesssim \|f\|, \quad \|u\|_2 \lesssim \|f\|.$$

3 C^0 finite element method Based on the modified mixed formulation, we propose a C^0 linear finite element method for the biharmonic problem (1.2), and derive the error estimates.

Denote by \mathcal{T}_h the triangulation of Ω . The C^0 -Lagrange finite element space V_h is given by

$$(3.1) \quad V_h := \{v \in C^0(\Omega) \cap V^1 : v|_K \subset P_1, \forall K \in \mathcal{T}_h\},$$

where P_1 denotes the space of linear polynomials on each element K .

We propose a C^0 finite element algorithm for the biharmonic problem (1.2) based on (2.21) in Algorithm 3.1.

Algorithm 3.1: C^0 finite element method

Step 1: *Solve for $w_h \in V_h$ from*

$$A(w_h, v_h) = (f, v_h), \quad \forall v_h \in V_h.$$

Step 2: *Solve for $\zeta_{m,h} \in V_h$, $1 \leq m \leq d_\perp$ from*

$$A(\zeta_{m,h}, v_h) = (\Delta(\chi s_m), v_h), \quad \forall v_h \in V_h,$$

where χ, s_m are given in Definition 2.3;

Compute $\xi_{m,h} = \zeta_{m,h} + \chi s_m$;

Step 3: *Compute the coefficients*

$$(3.2) \quad \Xi_h C_h = W_h,$$

where $\Xi_h \in \mathbb{R}^{d_\perp \times d_\perp}$ is the coefficient matrix with the mm' th entry $(\xi_{m,h}, \xi_{m',h})$,

$C_h = [c_{1,h}, \dots, c_{d_\perp,h}]^\top \in \mathbb{R}^{d_\perp}$, and $W_h \in \mathbb{R}^{d_\perp}$ with the m th entry $(w_h, \xi_{m,h})$.

Step 4: *Solve $u_h \in V_h$ from*

$$(3.3) \quad A(u_h, v_h) = \left(w_h - \sum_{m=1}^{d_\perp} c_{m,h} \xi_{m,h}, v_h \right), \quad \forall v_h \in V_h.$$

By the Lax-Milgram Theorem, the equations in Algorithm 3.1 are well-posed.

REMARK 3.1. By [Assumption 2.2](#), if $\ell \in \mathcal{D}^2 \cup \mathcal{N}^2$ for $\omega < \pi$ and $\ell \in \mathcal{M}' \cup \mathcal{M}''$ for $\omega \leq \frac{\pi}{2}$, the solution satisfies $u \in V^2$. For these cases, [Algorithm 3.1](#) reduces to the naive mixed finite element method.

REMARK 3.2. [Algorithm 3.1](#) extends naturally to the biharmonic equation with Neumann boundary conditions ($\Gamma_N = \partial\Omega$), which will be discussed in [Section 4](#), by substituting the finite element space V_h with \bar{V}_h defined in [\(4.9\)](#).

In every case, s_m in [\(2.9\)](#) has the form

$$s_m(r, \theta) = r^{-\beta_m} \Phi_m(\theta),$$

where $\beta_m > 0$ is the positive number appearing as the absolute value of the exponent of r in [\(2.9\)](#), Φ_m denotes an appropriate trigonometric functions. By the regularity theory for the Poisson equation in polygonal domains (see [19]), since w, ζ_m solve the Poisson problems [\(2.21\)](#), [\(2.10\)](#), we have

$$w, \zeta_m \in H^{1+\alpha}(\Omega),$$

where $\alpha := \min_m \beta_m - \varepsilon$, and $\varepsilon > 0$ is chosen sufficiently small. For simplicity of the error analysis below, we further assume that the solution exhibits a singular behavior characterized by $\alpha < 1$. Then, standard finite element error estimates yield the following result.

LEMMA 3.3. *Let w, ζ_m , and ξ_m be the solutions of [\(2.21\)](#), [\(2.10\)](#), and [\(2.8\)](#), respectively, and let $w_h, \zeta_{m,h}$, and $\xi_{m,h}$ be the corresponding finite element approximations in [Algorithm 3.1](#). Then,*

$$\begin{aligned} \|w - w_h\|_1 &\lesssim h^\alpha \|w\|_{1+\alpha}, \quad \|w - w_h\| \lesssim h^{2\alpha} \|w\|_{1+\alpha}, \\ \|\xi_m - \xi_{m,h}\|_1 &\lesssim h^\alpha \|\zeta_m\|_{1+\alpha}, \quad \|\xi_m - \xi_{m,h}\| \lesssim h^{2\alpha} \|\zeta_m\|_{1+\alpha}, \end{aligned}$$

where w and ζ_m satisfy the following regularity estimates:

$$\|w\|_{1+\alpha} \lesssim \|f\|, \quad \|\zeta_m\|_{1+\alpha} \lesssim \|\Delta(\chi s_m)\|.$$

LEMMA 3.4. *Let $\gamma > 0$ be a constant, and let p, q be bounded scalars. If $|p - p_h| \lesssim h^\gamma$, $|q - q_h| \lesssim h^\gamma$, then there exists $h_0 > 0$ such that for all $h < h_0$, the quantities p_h and q_h are uniformly bounded, and*

$$|pq - p_h q_h| \lesssim h^\gamma.$$

Proof. By assumption, there exists $C > 0$ such that $|p - p_h| \leq Ch^\gamma$ and $|q - q_h| \leq Ch^\gamma$ for all sufficiently small h . Choose $h_0 > 0$ such that $Ch_0^\gamma < 1$. Then for $h < h_0$,

$$|p_h| \leq |p| + |p - x_h| \leq |p| + 1, \quad |q_h| \leq |q| + |q - y_h| \leq |q| + 1,$$

so p_h and q_h are uniformly bounded.

Furthermore, it follows

$$|pq - p_h q_h| = |p(q - q_h) + (p - p_h)q_h| \leq |p| |q - q_h| + |p - p_h| |q_h|.$$

Using the bounds above, we obtain

$$|pq - p_h q_h| \leq |p| Ch^\gamma + Ch^\gamma (|q| + 1) \lesssim h^\gamma. \quad \square$$

In terms of the finite element approximation u_h in [Algorithm 3.1](#), we have the following result.

THEOREM 3.5. *Let u be the solution to the modified mixed formulation [\(2.22\)](#), and u_h be finite element approximation in [Algorithm 3.1](#). Then,*

$$(3.4) \quad \|u - u_h\|_1 \lesssim h^{\min\{1, 2\alpha\}}.$$

More specifically,

$$(3.5) \quad \|u - u_h\|_1 \lesssim \begin{cases} h^{2\alpha}, & \text{if } \ell \in \mathcal{M}' \cup \mathcal{M}'', \omega > \pi, \\ h, & \text{otherwise.} \end{cases}$$

Proof. Taking $\psi = v_h$ in (2.22b) and subtracting (3.3) from (2.22b) yield

$$(3.6) \quad A(u - u_h, v_h) = \left((w - \sum_{m=1}^{d_\perp} c_m \xi_m) - (w_h - \sum_{m=1}^{d_\perp} c_{m,h} \xi_{m,h}), v_h \right).$$

Let $u_I \in V_h$ denote the Lagrange interpolation of u onto V_h . Since $u \in V^2 \subset H^2(\Omega)$, the standard interpolation estimate on the triangulation \mathcal{T}_h [10] yields

$$\|u - u_I\|_1 \lesssim h \|u\|_2.$$

Denote $\varepsilon_h = u_I - u$ and $e_h = u_I - u_h$. By taking $v_h = e_h$ in (3.6), it follows

$$\begin{aligned} |e_h|_1^2 &= (\nabla \varepsilon_h, \nabla e_h) + (w - w_h, e_h) - \sum_{m=1}^{d_\perp} (c_m - c_{m,h})(\xi_m, e_h) - \sum_{m=1}^{d_\perp} c_{m,h}(\xi_m - \xi_{m,h}, e_h) \\ &\leq |\varepsilon_h|_1 |e_h|_1 + (\|w - w_h\| + \sum_{m=1}^{d_\perp} |c_m - c_{m,h}| \|\xi_m\| + \sum_{m=1}^{d_\perp} |c_{m,h}| \|\xi_m - \xi_{m,h}\|) \|e_h\| \\ &\lesssim \left(|\varepsilon_h|_1 + \|w - w_h\| + \sum_{m=1}^{d_\perp} |c_m - c_{m,h}| \|\xi_m\| + \sum_{m=1}^{d_\perp} |c_{m,h}| \|\xi_m - \xi_{m,h}\| \right) \|e_h\|_1. \end{aligned}$$

By Poincare's inequality [27],

$$\|e_h\|_1^2 \lesssim |e_h|_1^2 \lesssim (|\varepsilon_h|_1 + (\|w - w_h\| + \sum_{m=1}^{d_\perp} |c_m - c_{m,h}| \|\xi_m\| + \sum_{m=1}^{d_\perp} |c_{m,h}| \|\xi_m - \xi_{m,h}\|) \|e_h\|_1),$$

which implies

$$(3.7) \quad \|e_h\|_1 \lesssim |u - u_I|_1 + \|w - w_h\| + \sum_{m=1}^{d_\perp} |c_m - c_{m,h}| \|\xi_m\| + \sum_{m=1}^{d_\perp} |c_{m,h}| \|\xi_m - \xi_{m,h}\|.$$

By (2.20) and (3.2), the coefficients can be expressed as

$$c_m = \frac{1}{|\Xi|} \sum_{m'=1}^{d_\perp} \Xi_{(m',m)}(w, \xi_{m'}), \quad c_{m,h} = \frac{1}{|\Xi_h|} \sum_{m'=1}^{d_\perp} \Xi_{h,(m',m)}(w_h, \xi_{m',h}).$$

The notations $\Xi_{(m',m)}$ and $\Xi_{h,(m',m)}$ denote the algebraic cofactors of Ξ and Ξ_h , respectively. Specially, if $\dim \mathcal{S}^\perp = 1$, it holds $\Xi_{(1,1)} = \Xi_{h,(1,1)} = 1$.

By Lemma 3.3, there exists $h_0 > 0$ such that for all $h < h_0$, it holds $\|\xi_{m,h}\|_1 \leq \|\xi_m\|_1 + 1$ and $\|w_h\|_1 \leq \|w\|_1 + 1$. Note that for $m, m' \geq 1$,

$$(3.8) \quad \begin{aligned} |(\xi_m, \xi_{m'}) - (\xi_{m,h}, \xi_{m',h})| &= |(\xi_m, \xi_{m'} - \xi_{m',h}) + (\xi_m - \xi_{m,h}, \xi_{m',h})| \\ &\leq \|\xi_{m'} - \xi_{m',h}\| \|\xi_m\| + \|\xi_m - \xi_{m,h}\| \|\xi_{m',h}\| \lesssim h^{2\alpha}, \end{aligned}$$

$$(3.9) \quad \begin{aligned} |(w, \xi_{m'}) - (w_h, \xi_{m',h})| &\leq |(w, \xi_{m'} - \xi_{m',h}) + (w - w_h, \xi_{m',h})| \\ &\lesssim \|\xi_{m'} - \xi_{m',h}\| \|w\| + \|w - w_h\| \|\xi_{m',h}\| \lesssim h^{2\alpha}. \end{aligned}$$

Since each quantity $\Xi_{(m',m)}(w, \xi_{m'})$ and $|\Xi|$ is a linear combination of products of the terms $(\xi_m, \xi_{m'})$, $(w, \xi_{m'})$, and constants, it follows from Lemma 3.4 with $\gamma = 2\alpha$, together with (3.8) and (3.9), that

$$|\Xi_{(m',m)}(w, \xi_{m'}) - \Xi_{h,(m',m)}(w_h, \xi_{m',h})| \lesssim h^{2\alpha}, \quad ||\Xi| - |\Xi_h|| \lesssim h^{2\alpha}.$$

Then it follows

$$\begin{aligned}
|c_m - c_{m,h}| &= \left| \frac{1}{|\Xi|} \sum_{m'=1}^{d_\perp} \Xi_{(m',m)}(w, \xi_{m'}) - \frac{1}{|\Xi_h|} \sum_{m'=1}^{d_\perp} \Xi_{h,(m',m)}(w_h, \xi_{m',h}) \right| \\
&= \left| \frac{1}{|\Xi|} \sum_{m'=1}^{d_\perp} (\Xi_{(m',m)}(w, \xi_{m'}) - \Xi_{h,(m',m)}(w_h, \xi_{m',h})) + \left(\frac{1}{|\Xi|} - \frac{1}{|\Xi_h|} \right) \sum_{m'=1}^{d_\perp} \Xi_{h,(m',m)}(w_h, \xi_{m',h}) \right| \\
&\leq \frac{1}{|\Xi|} \sum_{m'=1}^{d_\perp} |\Xi_{(m',m)}(w, \xi_{m'}) - \Xi_{h,(m',m)}(w_h, \xi_{m',h})| + \frac{||\Xi_h| - |\Xi||}{|\Xi \Xi_h|} \sum_{m'=1}^{d_\perp} |\Xi_{h,(m',m)}(w_h, \xi_{m',h})| \\
&\lesssim h^{2\alpha}.
\end{aligned}$$

By [Lemma 3.4](#), $|c_{m,h}|$ is uniformly bounded. Substituting the estimate of $|c_m - c_{m,h}|$ into [\(3.7\)](#) gives

$$\begin{aligned}
\|u - u_h\|_1 &\lesssim \|u - u_I\|_1 + \|u_I - u_h\|_1 \\
&\lesssim \|u - u_I\|_1 + \|w - w_h\| + \sum_{m=1}^{d_\perp} |c_m - c_{m,h}| \|\xi_m\| + \sum_{m=1}^{d_\perp} |c_{m,h}| \|\xi_m - \xi_{m,h}\| \\
&\lesssim h^{\min\{1, 2\alpha\}},
\end{aligned}$$

which gives the estimate [\(3.5\)](#) as $\alpha < \frac{1}{2}$ when $\ell \in \mathcal{M}' \cup \mathcal{M}''$, $\omega > \pi$. \square

REMARK 3.6. We note that the error estimate for high-order approximations using P_k polynomials with $k \geq 2$ is not simply

$$\|u - u_h\|_1 \lesssim h^{\min\{k, 2\alpha\}},$$

as it can also be influenced by additional factors. A detailed investigation of these effects will be addressed in future research.

REMARK 3.7. In [Theorem 3.5](#), the predicted convergence rate is $h^{2\alpha}$ with $2\alpha < 1$ when the largest interior angle exceeds π and is associated with mixed boundary conditions. However, extensive numerical experiments consistently demonstrate the optimal convergence rate of h . This may be because the component of the solution influenced by the correction $c_2 \xi_2$ in w_S of the modified mixed formulation [\(2.21\)](#) is very small, although the correction remains necessary (see [Table 7](#) in [Example 5.4](#)).

4 Neumann boundary conditions Specifically, we consider the pure Neumann boundary case, that is, $\Gamma_D = \emptyset$, $\Gamma_N = \partial\Omega$. Then the biharmonic problem [\(1.2\)](#) reduces to

$$(4.1) \quad \begin{cases} \Delta^2 u = f & \text{in } \Omega, \\ \partial_{\mathbf{n}} u = \Delta \partial_{\mathbf{n}} u = 0 & \text{on } \partial\Omega. \end{cases}$$

The variational formulation of [\(4.1\)](#) is to find $u \in \bar{V}^2$ satisfying

$$(4.2) \quad a(u, v) = (f, v), \quad \forall v \in \bar{V}^2,$$

where $f \in L^2(\Omega)$ satisfies the compatibility $\int_{\Omega} f \, dx = 0$, and the Sobolev space \bar{V}^2 is defined by

$$\bar{V}^2 = \{v \in H^2(\Omega) : \partial_{\mathbf{n}} v|_{\partial\Omega} = 0, \int_{\Omega} v \, dx = 0\}.$$

Similar to the general boundary conditions discussed in [Subsection 2.1](#), the problem [\(4.1\)](#) can also be fully decomposed into the naive mixed formulation: two Poisson equations with Neumann boundary conditions

$$(4.3) \quad \begin{cases} -\Delta w = f & \text{in } \Omega, \\ \partial_{\mathbf{n}} w = 0 & \text{on } \partial\Omega, \end{cases} \quad \begin{cases} -\Delta \bar{u} = w & \text{in } \Omega, \\ \partial_{\mathbf{n}} u = 0 & \text{on } \partial\Omega. \end{cases}$$

The corresponding variational formulations are to find $\bar{u}, w \in \bar{V}^1$ such that

$$(4.4) \quad \begin{cases} A(w, \phi) = (f, \phi), & \forall \phi \in \bar{V}^1, \\ A(\bar{u}, \psi) = (w, \psi), & \forall \psi \in \bar{V}^1. \end{cases}$$

Here, the Sobolev space \bar{V}^1 is defined by

$$\bar{V}^1 = \{v \in H^1(\Omega) : \int_{\Omega} v \, dx = 0\}.$$

Note that $w \in \bar{V}^1$ implies $\int_{\Omega} w \, dx = 0$, which guarantees the well-posedness of the second Poisson problem subject to the Neumann boundary condition. The naive mixed formulation (4.3) suffers from the same issues as the schemes corresponding to other boundary conditions discussed earlier. In the following part, we will introduce the corresponding modified mixed formulation.

4.1 Modified mixed formulation We follow the same assumption for the domain as described in [Assumption 2.2\(i\)](#). Specially, it holds $d_{\perp} = 1$. The L^2 function ξ (for simplicity, we omit the subscript m in this section) is defined by

$$(4.5) \quad \xi = \chi s + \zeta, \quad s = r^{-\frac{\pi}{\omega}} \cos \frac{\pi}{\omega} \theta, \quad \begin{cases} -\Delta \zeta = \Delta(\chi s) & \text{in } \Omega, \\ \partial_{\mathbf{n}} \zeta = 0 & \text{on } \partial\Omega. \end{cases}$$

Here, ξ forms the basis function of the orthogonal space \mathcal{S}^{\perp} . Then, the modified mixed formuation is similarly given by

$$(4.6) \quad \begin{cases} -\Delta w = f & \text{in } \Omega, \\ \partial_{\mathbf{n}} w = 0 & \text{on } \partial\Omega, \end{cases} \quad \begin{cases} -\Delta \tilde{u} = w_{\mathcal{S}} & \text{in } \Omega, \\ \partial_{\mathbf{n}} \tilde{u} = 0 & \text{on } \partial\Omega, \end{cases}$$

where

$$(4.7) \quad w_{\mathcal{S}} = w - w_{\mathcal{S}^{\perp}}, \quad w_{\mathcal{S}^{\perp}} = \frac{(w, \xi)}{\|\xi\|^2} \xi.$$

The corresponding variational formulation is to find $\tilde{u}, w \in \bar{V}^1$ satisfying

$$(4.8) \quad \begin{cases} A(w, \phi) = (f, \phi), & \forall \phi \in \bar{V}^1, \\ A(\tilde{u}, \psi) = (w_{\mathcal{S}}, \psi), & \forall \psi \in \bar{V}^1. \end{cases}$$

LEMMA 4.1. *The modified mixed formulation (4.6) or (4.8) admits a unique solution $w, \tilde{u} \in \bar{V}^1$.*

Proof. Since f satisfies the compatibility condition, the existence and uniqueness of w are immediate. To establish the existence and uniqueness of \tilde{u} , it suffices to show that $w_{\mathcal{S}}$ in (4.7) satisfies the compatibility condition $\int_{\Omega} w_{\mathcal{S}} \, dx = \int_{\Omega} w \, dx - \frac{(w, \xi)}{\|\xi\|^2} \int_{\Omega} \xi \, dx = 0$. Since w satisfies $\int_{\Omega} w \, dx = 0$, it suffices to prove that $\int_{\Omega} \xi \, dx = 0$.

First, (4.5) admits a unique solution $\zeta \in \bar{V}^1$, which follows from $\Delta(\chi s) \in L^2(\Omega)$ and

$$\begin{aligned} \int_{\Omega} \Delta(\chi s) \, dx &= \int_{\Omega} (\partial_r^2 + r^{-1} \partial_r + r^{-2} \partial_{\theta}^2)(\chi r^{-\frac{\pi}{\omega}} \cos \frac{\pi}{\omega} \theta) \, dx \\ &= \int_0^R r(\partial_r^2 + r^{-1} \partial_r - \frac{\pi^2}{\omega^2})(\chi r^{-\frac{\pi}{\omega}}) \, dr \int_0^{\omega} \cos \frac{\pi}{\omega} \theta \, d\theta = 0. \end{aligned}$$

Then, it follows

$$\int_{\Omega} \xi \, dx = \int_{\Omega} \zeta + \chi r^{-\frac{\pi}{\omega}} \cos \frac{\pi}{\omega} \theta \, dx = \int_{\Omega} \zeta \, dx + \int_0^R \chi r^{1-\frac{\pi}{\omega}} \, dr \int_0^{\omega} \cos \frac{\pi}{\omega} \theta \, d\theta = 0. \quad \square$$

Similar to the general boundary cases, we have the following results.

THEOREM 4.2. *The solution \tilde{u} to the modified mixed formulation (4.6) is identical to the solution u of the biharmonic problem (4.1), i.e., $\tilde{u} = u \in \bar{V}^2$. Moreover, the solution (w, u) to the modified mixed formulation (4.6) also satisfies*

$$\|w\|_1 \lesssim \|f\|, \quad \|u\|_2 \lesssim \|f\|.$$

Similar to the finite element space V_h in (3.1), we introduce the C^0 -Lagrange finite element space

$$(4.9) \quad \bar{V}_h := \{v \in C^0(\Omega) \cap \bar{V}^1 : v|_K \subset P_1, \forall K \in \mathcal{T}_h\},$$

where P_1 denotes the space of linear polynomials on each element K . Then the C^0 finite element algorithm for the biharmonic problem (4.1) based on the modified mixed formulation (4.6) can also be given by Algorithm 3.1 with V_h replaced by \bar{V}_h .

For ζ, w in (4.5) and (4.6), it follows $w, \zeta \in H^{1+\alpha}(\Omega)$ with $\alpha = \frac{\pi}{\omega} - \varepsilon$.

THEOREM 4.3. *Let w_h, ξ_h, u_h be the finite element approximations of C^0 finite element algorithm for w, ξ, u in the modified mixed formulation (4.6). Then it holds*

$$\|w - w_h\|_1 \lesssim h^\alpha, \quad \|w - w_h\| \lesssim h^{2\alpha}, \quad \|\xi - \xi_h\|_1 \lesssim h^\alpha, \quad \|\xi - \xi_h\| \lesssim h^{2\alpha}, \quad \|u - u_h\|_1 \lesssim h.$$

5 Numerical Tests In this section, we present numerical experiments on several model problems to verify the effectiveness of the proposed C^0 finite element algorithm, namely Algorithm 3.1. **Domain shape** For convenience of presentation, we consider the domains listed in Figure 2, which are formed by removing parts of a square domain centered at the origin Q with side length 4.

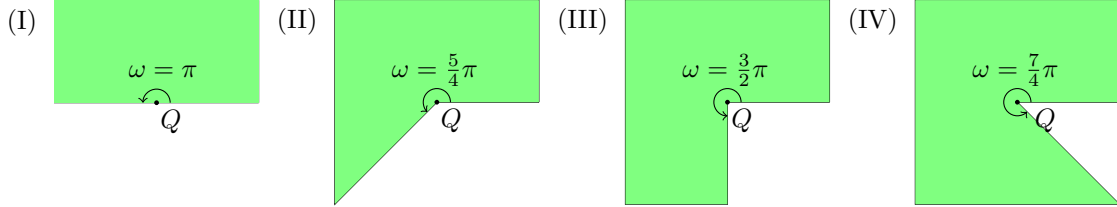


Figure 2: Four different polygonal domains used in the numerical experiments. The re-entrant corner at point Q has interior angle ω . I: $\omega = \pi$, II: $\omega = 5\pi/4$, III: $\omega = 3\pi/2$, IV: $\omega = 7\pi/4$.

Boundary conditions Boundary conditions are categorized into the following five types:

$$B_1 : \partial\Omega = \bar{\Gamma}_D; \quad B_2 : \tilde{\Gamma} \subset \bar{\Gamma}_D, \ell \in \mathcal{N}^2; \quad B_3 : \tilde{\Gamma} \subset \bar{\Gamma}_D, \ell \in \mathcal{M}'; \quad B_4 : \tilde{\Gamma} \subset \bar{\Gamma}_D, \ell \in \mathcal{M}''; \quad B_5 : \partial\Omega = \bar{\Gamma}_N,$$

where $\tilde{\Gamma}$ is defined in (2.7).

Cut-off function Following [24], we consider the cut-off function

$$\chi(r; \tau, R) = \begin{cases} 0, & r > R, \\ 1, & r < \tau R, \\ -\frac{3}{16} \left(\frac{2r}{R(1-\tau)} - \frac{1+\tau}{1-\tau} \right)^5 + \frac{5}{8} \left(\frac{2r}{R(1-\tau)} - \frac{1+\tau}{1-\tau} \right)^3 - \frac{15}{16} \left(\frac{2r}{R(1-\tau)} - \frac{1+\tau}{1-\tau} \right) + \frac{1}{2}. \end{cases}$$

For domains in Figure 2, we take $R = 1.8$, $\tau = 0.125$.

Since analytical solutions to these biharmonic problems are unavailable, we employ the C^0 interior penalty discontinuous Galerkin (C^0 -IPDG) method [3,5], which has been shown to produce numerical solutions that converge to the true solution independently of the geometry of Ω and the imposed boundary conditions. In our computations, we use P_2 Lagrange elements, and the penalty parameter is chosen according to the specific problem under consideration. After 7 uniform mesh refinements, the resulting numerical solution, denoted by u_R , is taken as the reference solution.

In addition, we denote by u_h^N the finite element solution based on the naive mixed formulation and by u_h^M the finite element solution from Algorithm 3.1. To compute the convergence rate, we employ the Cauchy numerical convergence rate $\mathcal{R}(j)$ for a generic finite element solution v_h , defined as

$$\mathcal{R}(j) = \log_2 \frac{|v_j - v_{j-1}|_1}{|v_{j+1} - v_j|_1}, \quad j \geq 1.$$

Here, v_j denotes the finite element solution v_h on the mesh \mathcal{T}_h obtained after j uniform refinements of the initial triangulation.

5.1 Mixed boundary conditions with $\Gamma_D \neq \emptyset$ For all numerical tests in this subsection, unless otherwise specified, we set $f \equiv 1$ in Ω .

Example 5.1. Consider domain I , $\Omega = [-2, 2] \times [0, 2]$, with boundary types B_3 and B_4 . The corresponding triangulation and mesh refinements are shown in Figure 3.

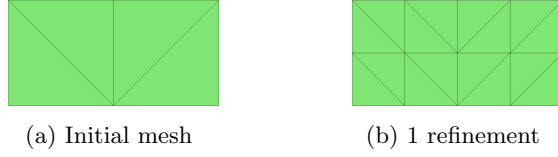


Figure 3: Example 5.1: Initial mesh and mesh after 1 refinement.

Consider the re-entrant corner $Q = Q_\ell$ with $\ell \in \mathcal{M}' \cup \mathcal{M}''$, having an interior angle $\omega = \pi$, located at the intersection of edges with Neumann and Dirichlet boundary conditions, respectively. In this case, $d_\perp = 1$. We compute the finite element solution u_h^N and u_h^M , with the reference solution obtained using the C^0 -IPDG method with penalty parameter $\sigma = 50$. The numerical solutions u_h^N and u_h^M , computed on a mesh after eight uniform refinements, along with their differences from the reference solution, are presented in Figure 4. The L^∞ norm of the differences $|u_R - u_h^N|$, $|u_R - u_h^M|$ after 3 to 6 refinements are presented in Table 1. From these results, we observe that the naive mixed finite element solution u_h^N converges to an incorrect solution, whereas the solution obtained from Algorithm 3.1 converges to the true solution.

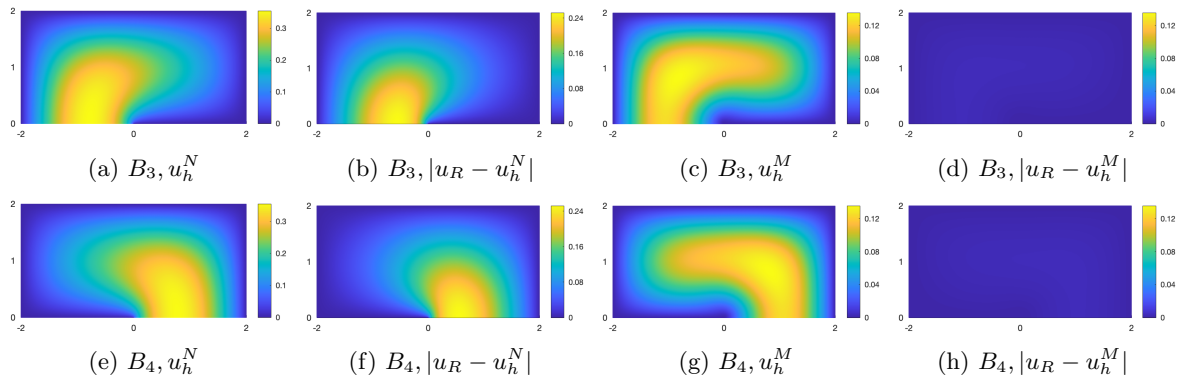


Figure 4: Example 5.1: Domain I; Boundary type: B_3, B_4 ; u_h^N, u_h^M and their differences with u_R .

The convergence rates of w_h and u_h^M are shown in Table 2. From these results, we observe that u_h^M exhibits a convergence rate of order h^1 , whereas the convergence rate of w_h approaches h^α with $\alpha = 0.5$ under boundary types B_3 and B_4 , which are consistent with the result in Lemma 3.3 and Theorem 3.5.

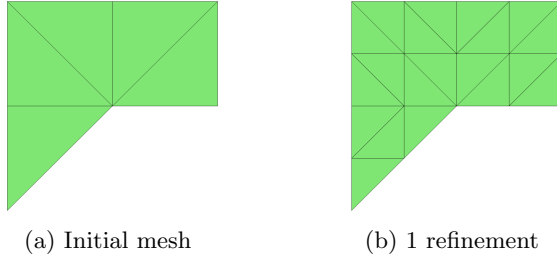
Table 1: [Example 5.1](#): Domain I, L^∞ errors.

	Boundary type	3	4	5	6
$\ u_R - u_h^N\ _\infty$	B_3	2.1000e-01	2.3616e-01	2.4758e-01	2.5287e-01
	B_4	2.0998e-01	2.3614e-01	2.4756e-01	2.5285e-01
$\ u_R - u_h^M\ _\infty$	B_3	7.7457e-03	4.0231e-03	1.8178e-03	1.2360e-03
	B_4	7.7340e-03	4.0151e-03	1.8098e-03	1.2210e-03

Table 2: [Example 5.1](#): Domain I, convergence rates of w_h, u_h^M .

	Boundary type	j=3	j=4	j=5	j=6	j=7	j=8
\mathcal{R} for u_h^M	B_3	0.82	0.91	0.97	0.99	0.99	1.00
	B_4	0.82	0.91	0.97	0.99	0.99	1.00
\mathcal{R} for w_h	B_3	0.77	0.76	0.70	0.63	0.57	0.54
	B_4	0.77	0.76	0.70	0.63	0.57	0.54

Example 5.2. We repeat [Example 5.1](#) in domain II, $\Omega = [-2, 2]^2 \setminus \{(x, y) | y < 0, y < x\}$, with boundary types B_3 and B_4 . The initial mesh and the mesh after one refinement are shown in [Figure 5](#).

Figure 5: [Example 5.2](#): Initial mesh and mesh after 1 refinement.

In this case, the largest interior angle $\omega = \frac{5}{4}\pi$, and $d_\perp = 1$. The numerical solutions u_h^N and u_h^M , computed on a mesh after eight uniform refinements, along with their differences from the reference solution, are presented in [Figure 6](#). The L^∞ norm of the differences $|u_R - u_h^N|$, $|u_R - u_h^M|$ after 3 to 6 refinements are presented in [Table 3](#). From these results, we further observe that the naive mixed finite element solution u_h^N converges to an incorrect solution, whereas the solution obtained from [Algorithm 3.1](#) converges to the true solution.

Table 3: [Example 5.2](#): Domain II, L^∞ errors.

	Boundary type	3	4	5	6
$\ u_R - u_h^N\ _\infty$	B_3	2.6724e-01	3.0462e-01	3.2480e-01	3.3618e-01
	B_4	2.6306e-01	3.0116e-01	3.2253e-01	3.3407e-01
$\ u_R - u_h^M\ _\infty$	B_3	8.4341e-03	3.9003e-03	1.6030e-03	1.0728e-03
	B_4	8.1807e-03	3.8357e-03	1.5541e-03	1.0044e-03

The convergence rates of w_h and u_h^M are shown in [Table 4](#). From these results, we observe that u_h^M exhibits a convergence rate of order h^1 , whereas the convergence rate of w_h approaches h^α with $\alpha = 0.4$ under boundary types B_3 and B_4 , which are consistent with the result in [Lemma 3.3](#) and [Theorem 3.5](#).

Example 5.3. Consider the L-shaped domain III, $\Omega = [-2, 2]^2 \setminus \{(x, y) | x > 0, y < 0\}$; the initial mesh and the mesh after 1 refinement are shown in [Figure 7](#). This domain contains an interior angle of $\frac{3}{2}\pi$; we examine boundary types B_1, B_2, B_3 , and B_4 , with $d_\perp = 1$ for all cases. For these four cases,

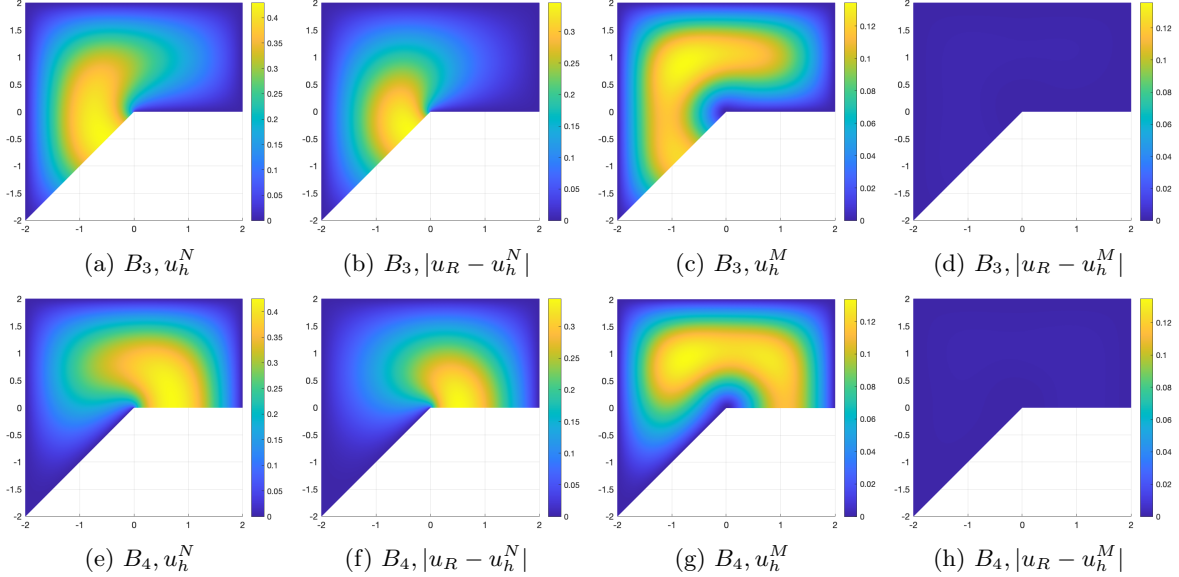


Figure 6: [Example 5.2](#): Domain II; Boundary type: B_3, B_4 ; u_h^N, u_h^M and their differences with u_R .

Table 4: [Example 5.2](#): Domain II, convergence rates of w_h, u_h^M .

	Boundary type	j=3	j=4	j=5	j=6	j=7	j=8
\mathcal{R} for u_h^M	B_3	0.83	0.91	0.97	0.99	0.99	1.00
	B_4	0.83	0.91	0.97	0.99	0.99	1.00
\mathcal{R} for w_h	B_3	0.72	0.67	0.58	0.50	0.45	0.42
	B_4	0.73	0.66	0.57	0.49	0.45	0.42

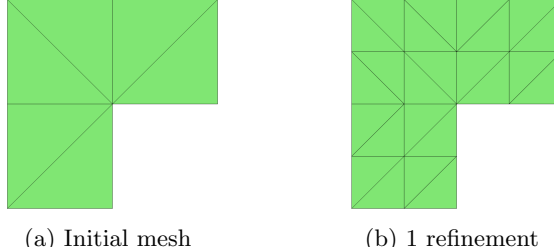


Figure 7: [Example 5.3](#): Initial mesh and mesh after 1 refinement.

we compute the finite element solution u_h^N and u_h^M , with the reference solution u_R obtained using the C^0 -IPDG method with penalty parameter $\sigma = 32, 160, 50, 50$, respectively. The numerical solutions u_h^N and u_h^M , computed on a mesh after eight uniform refinements, along with their differences from the reference solution, are presented in [Figure 8](#) for boundary types B_1 and B_2 , and [Figure 9](#) or boundary types B_3 and B_4 . The L^∞ norm of $|u_R - u_h^N|$, $|u_R - u_h^M|$ after 3 to 6 times refinements of the mesh are presented in [Table 5](#). From these results, we also observe that the naive mixed finite element solution u_h^N converges to an incorrect solution in all cases except when the boundary type is B_2 , whereas the solution obtained from [Algorithm 3.1](#) converges to the true solution.

The convergence rates of w_h and u_h^M are shown in [Table 6](#). From these results, we observe that u_h^M exhibits a convergence rate of order h^1 , whereas the convergence rate of w_h approaches h^α , with $\alpha = 2/3$ for boundary types B_1 and B_2 , and $\alpha = 1/3$ for boundary types B_3 and B_4 . These observations are consistent with the results in [Lemma 3.3](#) and [Theorem 3.5](#).

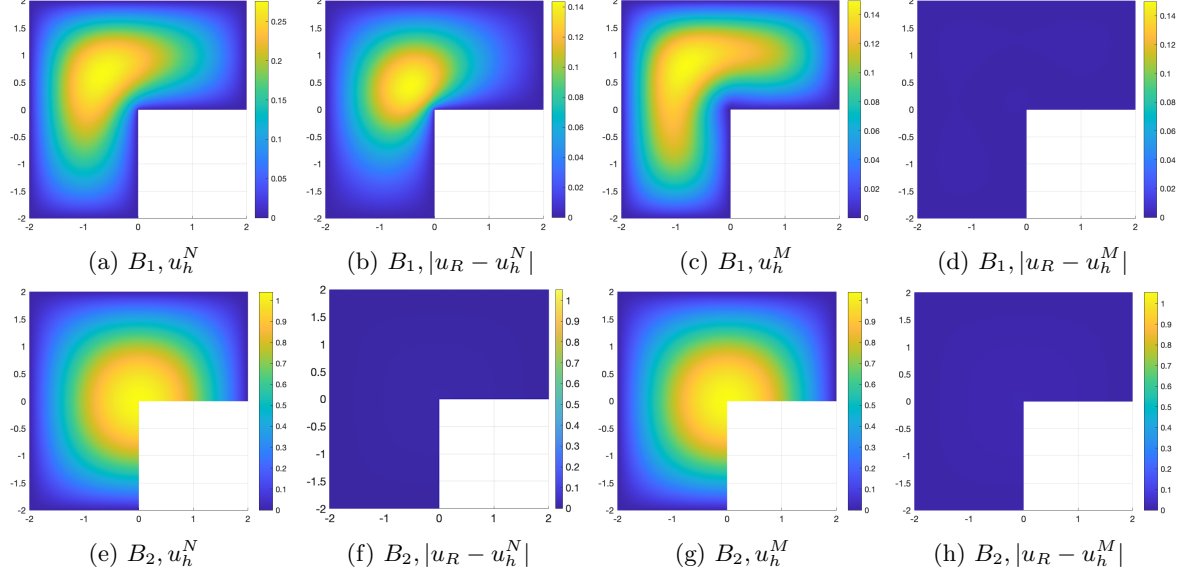


Figure 8: **Example 5.3:** Domain III; Boundary type: B_1, B_2 ; u_h^N, u_h^M and their differences with u_R .

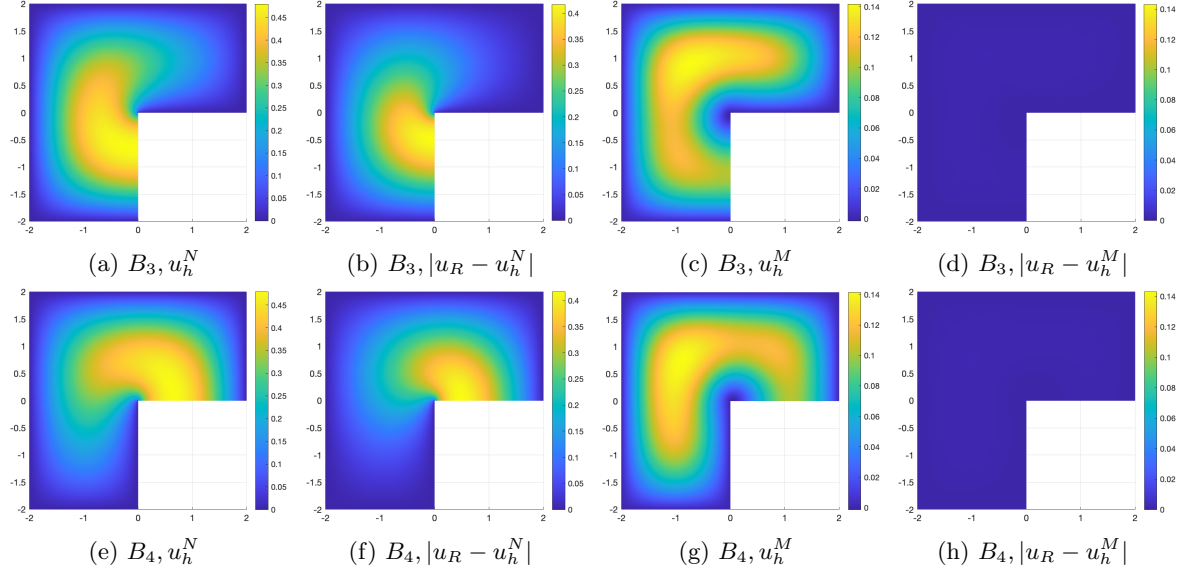


Figure 9: **Example 5.3:** Domain III; Boundary type: B_3, B_4 ; u_h^N, u_h^M and their differences with u_R .

Table 6: **Example 5.3:** Domain III, convergence rates of w_h, u_h^M .

	Boundary type	j=3	j=4	j=5	j=6	j=7	j=8
\mathcal{R} for u_h^M	B_1	0.84	0.92	0.97	0.99	0.99	1.00
	B_2	0.86	0.96	0.99	1.00	1.00	1.00
	B_3	0.83	0.92	0.97	0.99	1.00	1.00
	B_4	0.83	0.92	0.97	0.99	1.00	1.00
\mathcal{R} for w_h	B_1	0.83	0.88	0.87	0.84	0.80	0.77
	B_2	0.86	0.96	0.99	1.00	1.00	1.00
	B_3	0.69	0.62	0.51	0.43	0.38	0.36
	B_4	0.69	0.62	0.51	0.43	0.38	0.36

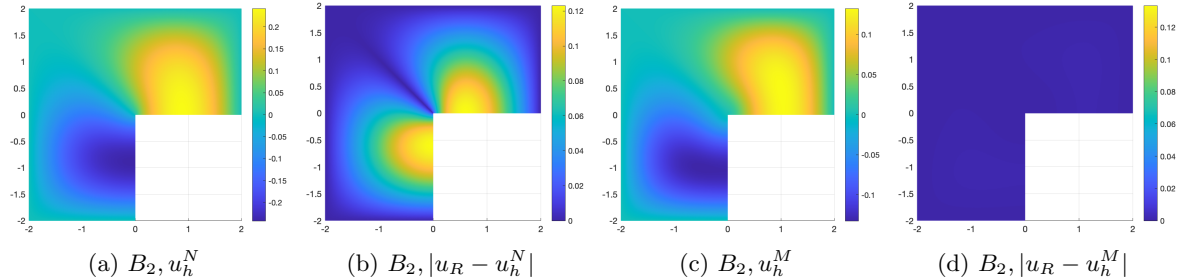
Table 5: **Example 5.3:** Domain III, L^∞ errors.

	Boundary type	3	4	5	6
$\ u_R - u_h^N\ _\infty$	B_1	1.2837e-01	1.3782e-01	1.4183e-01	1.4305e-01
	B_2	1.4597e-02	4.5660e-03	2.1383e-03	1.8196e-03
	B_3	3.0181e-01	3.5064e-01	3.8071e-01	3.9915e-01
	B_4	3.0180e-01	3.5063e-01	3.8071e-01	3.9914e-01
$\ u_R - u_h^M\ _\infty$	B_1	5.8104e-03	3.4371e-03	1.6673e-03	9.4410e-04
	B_2	1.4597e-02	4.5660e-03	2.1383e-03	1.8196e-03
	B_3	1.0371e-02	4.7030e-03	1.9051e-03	1.0291e-03
	B_4	1.0368e-02	4.7012e-03	1.9053e-03	1.0273e-03

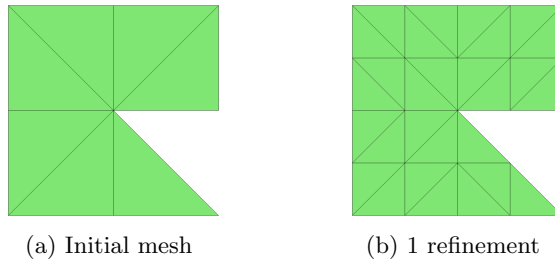
From [Figure 8](#), we observe that $|u_R - u_h^N| \rightarrow 0$ as mesh is refined for the boundary type B_2 , implying that Poisson's problem with $f \equiv C$ (with C being some constant) admits a weak solution $w \in \mathcal{S}$. Therefore, we consider a new source term $f \in L^2(\Omega)$ defined as follows:

$$(5.1) \quad f = \begin{cases} 1, & x \geq 0, y \geq 0, \\ 0, & x < 0, y \geq 0, \\ -1, & y < 0. \end{cases}$$

We repeat the numerical test, and report the solutions in [Figure 10](#), from which we observe that the naive mixed finite element solution u_h^N converges to an incorrect solution, while the solution obtained from [Algorithm 3.1](#) converges to the true solution.

Figure 10: **Example 5.3:** Domain III; Boundary type: B_2 ; f satisfies (5.1); u_h^N, u_h^M and differences.

Example 5.4. Consider domain IV, $\Omega = [-2, 2]^2 \setminus \{(x, y) \mid -x < y < 0\}$, with the initial mesh and the mesh after 1 refinement in [Figure 11](#). The boundary conditions are specified as B_3 and B_4 .

Figure 11: **Example 5.4:** Initial mesh and mesh after 1 refinement.

The largest interior angle is $\frac{7}{4}\pi$, and $d_\perp = 2$. We consider f given in (5.1). We compute the naive mixed finite element solution u_h^{N*} ; the modified mixed finite element solution u_h^{M*} from [Algorithm 3.1](#) with $d_\perp = 1$; and the modified mixed finite element solution u_h^M from [Algorithm 3.1](#) with $d_\perp = 2$. The reference solution is obtained using the C^0 -IPDG method with penalty parameter $\sigma = 68$.

The numerical solutions u_h^N , u_h^{M*} , and u_h^M , computed on a mesh after eight uniform refinements, along with their differences from the reference solution, are presented in Figure 12. The L^∞ norm of differences after 3 to 6 times refinements of the mesh are presented in Table 7. From these results, we observe that the finite element solutions u_h^N and u_h^{M*} converge to incorrect solutions, whereas the solution obtained from Algorithm 3.1 with $d_\perp = 2$ converges to the true solution, thereby confirming the necessity of properly accounting for the dimension of the orthogonal complement in the modified formulation.

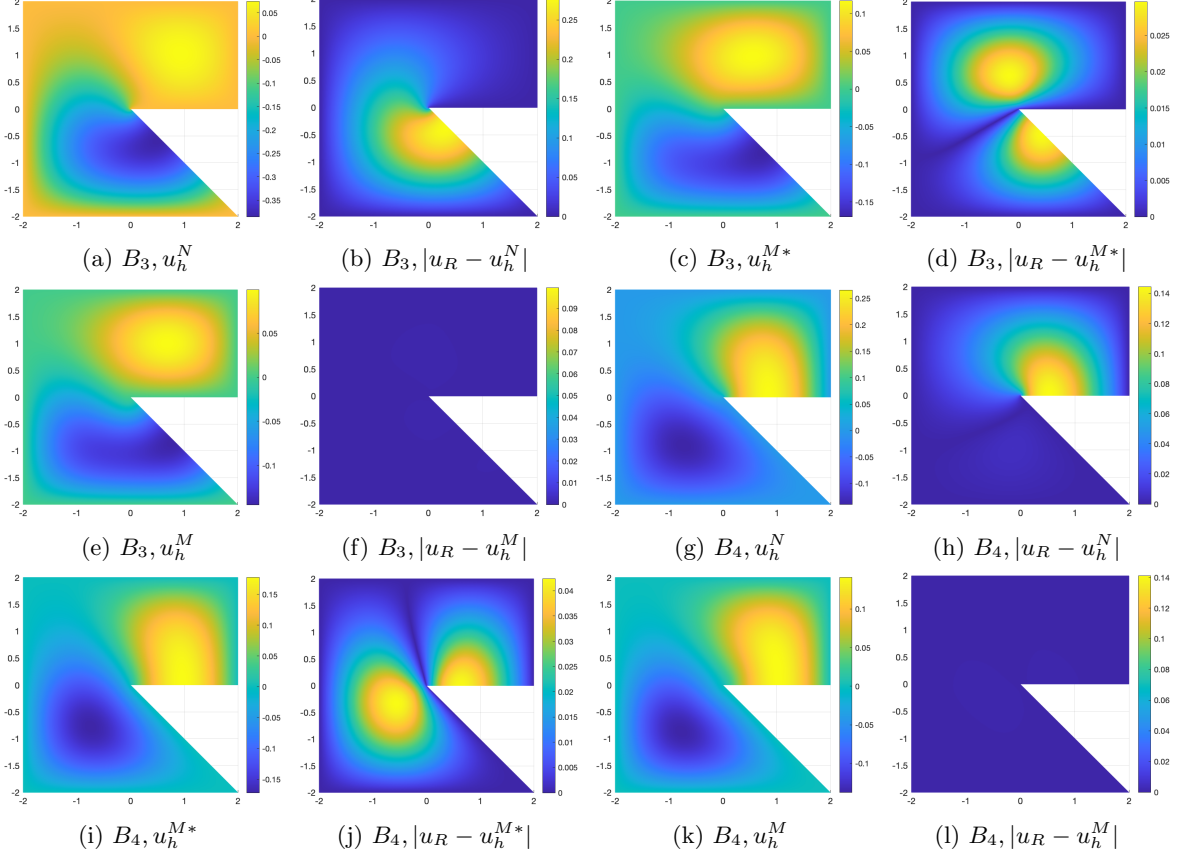


Figure 12: Example 5.4: Domain IV; Boundary type: B_3, B_4 ; u_h^N, u_h^{M*}, u_h^M and differences.

Table 7: Example 5.4: Domain IV, L^∞ errors.

	Boundary type	3	4	5	6
$\ u_R - u_h^N\ _\infty$	B_3	1.9797e-01	2.3068e-01	2.5019e-01	2.6279e-01
	B_4	1.0727e-01	1.2388e-01	1.3283e-01	1.3816e-01
$\ u_R - u_h^{M*}\ _\infty$	B_3	2.8418e-02	2.9444e-02	2.9573e-02	2.9527e-02
	B_4	3.8119e-02	4.1158e-02	4.1791e-02	4.2073e-02
$\ u_R - u_h^M\ _\infty$	B_3	6.4356e-03	3.1130e-03	1.2959e-03	7.3513e-04
	B_4	6.9425e-03	2.2060e-03	9.6986e-04	7.5067e-04

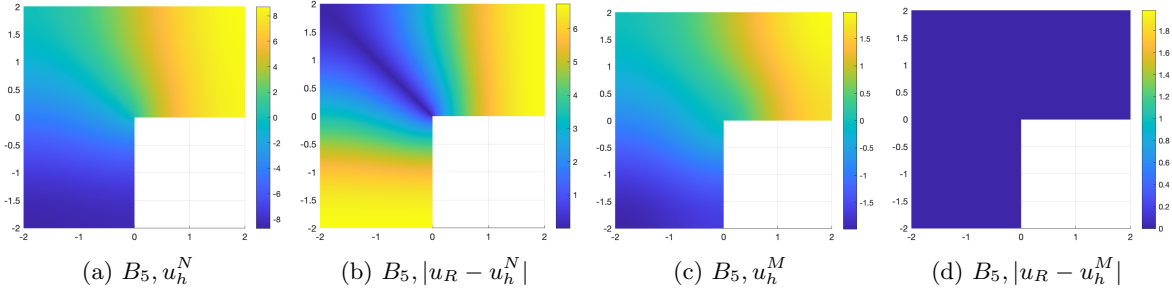
The convergence rates of w_h and u_h^M are shown in Table 8. From these results, we observe that u_h^M exhibits a convergence rate of order h^1 , whereas the convergence rate of w_h approaches h^α with $\alpha = 2/7$ under boundary types B_3 and B_4 .

Table 8: [Example 5.4](#): Domain IV, convergence rates of w_h, u_h^M .

	Boundary type	j=3	j=4	j=5	j=6	j=7	j=8
\mathcal{R} for u_h^M	B_3	0.83	0.92	0.97	0.99	1.00	1.00
	B_4	0.83	0.92	0.97	0.99	1.00	1.00
\mathcal{R} for w_h	B_3	0.67	0.58	0.47	0.38	0.33	0.31
	B_4	0.67	0.57	0.46	0.38	0.33	0.31

5.2 Neumann boundary conditions We consider the Neumann boundary conditions discussed in [Section 4](#).

Example 5.5. Consider domain III , $\Omega = [-2, 2]^2 \setminus \{(x, y) | x > 0, y < 0\}$, with boundary type B_5 . We take f as [\(5.1\)](#), which satisfies the compatibility condition $\int_{\Omega} f \, dx = 0$. For the reference solution, the mesh-dependent problem requires the functions in V_h to vanish at the origin. The interior penalty parameter is set to $\sigma = 39$. The triangulation and the mesh after 1 refinement are the same as in [Example 5.3](#). For this polygonal domain, there exists an interior angle of $\frac{3}{2}\pi$, and $d_{\perp} = 1$. The numerical solutions u_h^N and u_h^M , computed on a mesh after eight uniform refinements, along with their differences from the reference solution, are presented in [Figure 13](#). The L^{∞} norm of the differences $|u_R - u_h^N|$, $|u_R - u_h^M|$ after 3 to 6 refinements are presented in [Table 9](#). From these results, we observe that the naive mixed finite element solution u_h^N converges to an incorrect solution, whereas the solution obtained from Algorithm [3.1](#) with V_h replaced by \bar{V}_h in [\(4.9\)](#) converges to the true solution.

Figure 13: [Example 5.5](#): Domain III; Boundary type: B_5 ; f satisfies [\(5.1\)](#); u_h^N, u_h^M and differences.Table 9: [Example 5.5](#): Domain III, L^{∞} errors.

	Boundary type	3	4	5	6
$\ u_R - u_h^N\ _{\infty}$	B_5	6.5195e+00	6.6456e+00	6.6964e+00	6.7209e+00
$\ u_R - u_h^M\ _{\infty}$	B_5	3.8229e-02	1.7219e-02	8.0944e-03	6.4859e-03

The convergence rates of w_h and u_h^M are shown in [Table 10](#). From these results, we observe that u_h^M exhibits a convergence rate of order h^1 , whereas the convergence rate of w_h approaches h^{α} with $\alpha = 2/3$ under boundary type B_5 , which are consistent with the result in [Theorem 4.3](#).

Table 10: [Example 5.5](#): Domain III, convergence rates of w_h, u_h^M .

	Boundary type	j=3	j=4	j=5	j=6	j=7	j=8
\mathcal{R} for u_h^M	B_5	0.85	0.96	0.96	0.98	0.99	0.99
\mathcal{R} for w_h	B_5	0.73	0.73	0.72	0.70	0.69	0.68

Acknowledgments H. Li was supported in part by the National Science Foundation Grant DMS-2208321 and a Japan Society for the Promotion of Science Research Grant. N. Yi was supported by the National Key R & D Program of China (2024YFA1012600) and NSFC (12431014). P. Yin's research was supported by the University of Texas at El Paso Startup Award.

REFERENCES

- [1] BABUŠKA, I., OSBORN, J., AND PITKÄRANTA, J. Analysis of mixed methods using mesh dependent norms. *Mathematics of Computation* 35, 152 (1980), 1039–1062.
- [2] BRENNER, S. C. *The mathematical theory of finite element methods*. Springer, 2008.
- [3] BRENNER, S. C. C^0 interior penalty methods. In *Frontiers in Numerical Analysis-Durham 2010*. Springer, 2011, pp. 79–147.
- [4] BRENNER, S. C., MONK, P., AND SUN, J. C^0 interior penalty Galerkin method for biharmonic eigenvalue problems. In *Spectral and High Order Methods for Partial Differential Equations ICOSAHOM 2014: Selected papers from the ICOSAHOM conference, June 23–27, 2014, Salt Lake City, Utah, USA* (2015), Springer, pp. 3–15.
- [5] CAO, H., HUANG, Y., YI, N., AND YIN, P. A posteriori error estimators for fourth order elliptic problems with concentrated loads. *Journal of Scientific Computing* 105, 2 (2025), 1–41.
- [6] CHENG, X.-L., HAN, W., AND HUANG, H.-C. Some mixed finite element methods for biharmonic equation. *Journal of computational and applied mathematics* 126, 1-2 (2000), 91–109.
- [7] CIARLET, P., AND GLOWINSKI, R. Dual iterative techniques for solving a finite element approximation of the biharmonic equation. *Computer Methods in Applied Mechanics and Engineering* 5, 3 (1975), 277–295.
- [8] CIARLET, P. G. *The finite element method for elliptic problems*. SIAM, 2002.
- [9] CIARLET, P. G., AND RAVIART, P.-A. A mixed finite element method for the biharmonic equation. In *Mathematical aspects of finite elements in partial differential equations*. Elsevier, 1974, pp. 125–145.
- [10] CIARLET JR, P., AND HE, J. The singular complement method for 2d scalar problems. *Comptes Rendus Mathématique* 336, 4 (2003), 353–358.
- [11] COURANT, R., AND HILBERT, D. *Methods of mathematical physics, volume 1*, vol. 1. John Wiley & Sons, 2008.
- [12] DE COSTER, C., NICIAISE, S., AND SWEERS, G. Comparing variational methods for the hinged kirchhoff plate with corners. *Mathematische Nachrichten* 292, 12 (2019), 2574–2601.
- [13] DESTUYNDER, P., AND SALAUN, M. *Mathematical Analysis of Thin Plate Models*, vol. 24 of *Mathématiques & Applications (Berlin) [Mathematics & Applications]*. Springer-Verlag, Berlin, 1996.
- [14] DESTUYNDER, P., AND SALAUN, M. *Mathematical analysis of thin plate models*, vol. 24. Springer Science & Business Media, 2013.
- [15] FALK, R. S. Approximation of the biharmonic equation by a mixed finite element method. *SIAM Journal on Numerical Analysis* 15, 3 (1978), 556–567.
- [16] GALLISTL, D. Stable splitting of polyharmonic operators by generalized stokes systems. *Mathematics of Computation* 86, 308 (2017), 2555–2577.
- [17] GEORGULIS, E. H., AND HOUSTON, P. Discontinuous galerkin methods for the biharmonic problem. *IMA journal of numerical analysis* 29, 3 (2009), 573–594.
- [18] Gerasimov, T., Stylianou, A., And SWEERS, G. Corners give problems when decoupling fourth order equations into second order systems. *SIAM Journal on Numerical Analysis* 50, 3 (2012), 1604–1623.
- [19] GRISVARD, P. *Singularities in Boundary Value Problems*. Recherches en mathématiques appliquées. Masson, 1992.
- [20] HU, J., MA, R., AND ZHANG, M. A family of mixed finite elements for the biharmonic equations on triangular and tetrahedral grids. *Science China Mathematics* 64, 12 (2021), 2793–2816.
- [21] LI, H., WICKRAMASINGHE, C. D., AND YIN, P. Analysis of a C^0 finite element method for the biharmonic problem with dirichlet boundary conditions. *Numerical Algorithms* (2025), DOI:<https://doi.org/10.1007/s11075-025-02062-4>.
- [22] LI, H., AND YANG, Y. Adaptive morley element algorithms for the biharmonic eigenvalue problem. *Journal of Inequalities and Applications* 2018, 1 (2018), 55.
- [23] LI, H., AND YIN, P. A C^0 finite element algorithm for the sixth order problem with simply supported boundary conditions. *Numerical Methods for Partial Differential Equations* 41, 6 (2025), e70048.
- [24] LI, H., YIN, P., AND ZHANG, Z. A C^0 finite element method for the biharmonic problem with Navier boundary conditions in a polygonal domain. *IMA Journal of Numerical Analysis* 43, 3 (2023), 1779–1801.
- [25] MARDANOV, R., AND ZARIPOV, S. Solution of stokes flow problem using biharmonic equation formulation and multiquadratics method. *Lobachevskii Journal of Mathematics* 37 (2016), 268–273.
- [26] MATEVOSSIAN, H., NIKABADZE, M., AND ULUKHANYAN, A. ‘biharmonic problems and their applications. *Global J. Eng. Sci. Res* 6, 3 (2019), 263–272.
- [27] MEYERS, N. G. Integral inequalities of poincaré and wirtinger type. *Archive for Rational Mechanics and Analysis* 68, 2 (1978), 113–120.
- [28] MONK, P. A mixed finite element method for the biharmonic equation. *SIAM Journal on Numerical Analysis* 24, 4 (1987), 737–749.
- [29] NAZAROV, S., AND PLAMENEVSKY, B. A. Elliptic problems in domains with piecewise smooth boundaries, 1994.
- [30] NAZAROV, S., AND SVIRS, G. K. Boundary value problems for the biharmonic equation and the iterated Laplacian in a three-dimensional domain with an edge. *Zap. Nauchn. Sem. S.-Peterburg. Otdel. Mat. Inst. Steklov. (POMI)* 336, Kraev. Zadachi Mat. Fiz. i Smezh. Vopr. Teor. Funkts. 37 (2006), 153–198, 276–277.
- [31] NAZAROV, S., AND SWEERS, G. A boundary-value problem for the biharmonic equation and the iterated laplacian in a 3d-domain with an edge. *Journal of Mathematical Sciences* 143 (2007), 2936–2960.
- [32] RACHH, M., AND SERKH, K. On the solution of the stokes equation on regions with corners. *Communications on Pure and Applied Mathematics* 73, 11 (2020), 2295–2369.
- [33] RAFETSEDER, K., AND ZULEHNER, W. A decomposition result for kirchhoff plate bending problems and a new discretization approach. *SIAM Journal on Numerical Analysis* 56, 3 (2018), 1961–1986.

- [34] SOKOLNIKOFF, I. S. Mathematical theory of elasticity.
- [35] SWEERS, G. A survey on boundary conditions for the biharmonic. *Complex Var. Elliptic Equ.* 54, 2 (2009), 79–93.
- [36] TAIBAOUI, M. *A C^1 finite element method for the biharmonic problem*. PhD thesis, KASDI MERBAH UNIVERSITY OUARGLA.
- [37] TIMOSHENKO, S. Theory of plates and shells. *McGRAWC HILL* (1959).
- [38] UGURAL, A. C. *Stresses in beams, plates, and shells*. CRC press, 2009.
- [39] ZHANG, S., AND ZHANG, Z. Invalidity of decoupling a biharmonic equation to two poisson equations on non-convex polygons. *Int. J. Numer. Anal. Model.* 5, 1 (2008), 73–76.